EXPERIMENTAL METHODOLOGY FOR THE STUDY OF NATURAL CONVECTION ON FLAT AND CORRUGATED PLATES

S. A. Verdério Júnior[a],

V. L. Scalon[b],

S. R. Oliveira[c],

E. Avallone[d],

P. C. Mioralli[e],

D. M. Gonçalves[f]

Instituto Federal de Educação, Ciência e Tecnologia de São Paulo (IFSP)
Department of Industry,
CEP 14804-296, Araraquara, SP, Brazil
[a]silvioverderio@ifsp.edu.br,
[f]danieldamotta@ifsp.edu.br
CEP 15808-305, Catanduva, SP, Brazil
[d]elson.avallone@ifsp.edu.br
[e]mioralli@ifsp.edu.br

Universidade Estadual Paulista "Júlio de Mesquita Filho" (UNESP)
Faculdade de Engenharia de Bauru (FEB)
Department of Mechanical Engineering
CEP 17033-360, Bauru, SP, Brazil
[b]vicente.scalon@unesp.br,
[c]santiago.oliveira@unesp.br

Received: Jan 16, 2022
Revised: Jan 20, 2022
Accepted: Jan 25, 2022

ABSTRACT

Natural convection is present in the most different Thermal Engineering systems, such as solar collectors, electric furnaces, electronic equipment cooling, lubrication, thermal comfort projects in buildings, etc. In the last decade, the number of research on natural convection heat transfer has increased considerably, especially in the areas of physical-numerical modeling and validation, experimental construction and efficiency optimization of thermal systems, and related technologies. This work presents an experimental methodology for studying natural convection on flat and corrugated plates. The design and construction stages of the experimental apparatus, data processing and analysis, physical-mathematical modeling and uncertainty analysis were extensively explored. The applications and extensions of the proposed methodology were discussed in the numerical-experimental validation of physical-numerical modeling methodologies, design and optimization of the experimental apparatus and also of measuring instruments and, finally, in sensitivity analysis studies to reduce the propagation of uncertainties. The limitations of the proposed methodology were discussed, pointing out suggestions for future work.

Keywords: experimental methodology; natural convection; physical-mathematical modeling; heat transfer.

NOMENCLATURE

A	surface area, m²
A_P	projected area of thermal radiation heat exchange, m²
Bi	Biot number
c_{Al}	aluminum alloy specific heat capacity, J/(kg.K)
C	empirical constant
C_t	empirical coefficient of the exponential interpolation curves
$\mathbf{g}$	gravity acceleration, m/s²
$\bar{h}_{conv}$	average convective heat transfer coefficient, W/(m².K)
$\bar{h}_{rad}$	average thermal radiation heat transfer coefficient, W/(m².K)
$\bar{h}_{total}$	average total heat transfer coefficient, W/(m².K)
$k_{t_{Al}}$	aluminum alloy thermal conductivity, W/(m. K)
$k_{t_{fluid}}$	air thermal conductivity, W/(m. K)
L_P	plate longitudinal length, m
m_P	plate mass, kg
n	empirical coefficient
N	number of temperature sensors on plate
$\overline{Nu}$	average Nusselt number
Pr	Prandtl number
Q_{conv}	convection heat flow, W
Q_{rad}	thermal radiation heat flow, W
Ra	Rayleigh number
t	time, s
t_{eq}	time interval for homogenization of temperatures on the plate, s
T	temperature, K
$\overline{T}_f$	film temperature, K
T_{nb}	neighborhood temperature, K
T_P	plate temperature, K
T_S	surface temperature, K
T_∞	free-stream temperature, K

Greek symbols

δ	measurement uncertainty
ε	emissivity
Δt	time interval, s
ΔT	temperature difference, K
ν	kinematic viscosity, m²/s
σ	Stefan-Boltzmann constant, $W/(m^2.K^4)$

Superscripts

$\bar{}$	average value

Subscripts

final	relative to the final time
i	counter
initial	relative to the initial time
L_P	plate longitudinal length as characteristic length

INTRODUCTION

Natural convection occurs through self-induced movements (without external driving forces), due to temperature gradients and/or mass concentration gradients. It can be classified into internal or external natural convection. Unlike forced convection, it presents governing equations with strong mathematical coupling in mass transport and temperatures, presenting lower convection heat transfer coefficient and higher thermal resistance (Bejan, 2013; Bergman et al., 2014; Balaji et al., 2021).

Since the classic experimental study by Fishenden and Saunders (1965) and the proposition of the famous empirical correlation $\overline{Nu} = C.Ra^n$, the researches and applications of natural convection have been growing significantly.

The main applications and current trends of research involving natural convection are presented below, according to the studies by Saha et al. (2016), Sheikholeslami (2019), Balaji et al. (2021) and Izadi and Assad (2021).

Among the practical examples of natural convection in Thermal Engineering are applications in electric furnaces, cooling of electronic equipment (such as electrical transformers), lubrication systems, heat exchangers, solar collectors, solar water desalination, design of nuclear reactors cooling systems, etc.

Current research is being done in natural convection heat transfer in nanofluids, porous media, micropolar fluids, non-Newtonian fluids, etc. Studies of natural convection under the influence of magnetic fields have grown considerably in recent years, emphasizing industrial applications of crystal growth, metal casting, liquid metal cooling blankets for fusion reactors, etc.

In the last decade, considerable advances have been made in the applied study of natural convection; especially in the areas of computational physical-numerical modeling, experimental methodologies and optimization strategies and of greater applicability in modern thermal engineering systems. Such advances are shown in the studies of: Kitamura *et al.* (2015), in the presentation of empirical correlations of the type $\overline{Nu}$ x Ra, in different flow regimes, for natural convection in horizontal flat plates; Frank et al. (2019), in the application of combined heat transfer by natural convection and thermal radiation in the cooling of electronic components; Verdério Júnior et al. (2021a) and Verdério Júnior et al. (2021b), in the proposal and experimental validation of a numerical methodology for the study of natural convection, in turbulent and laminar regimes, on isothermal square flat plates; Silva et al. (2021), in the numerical-computational study and experimental validation of two different mesh configurations for turbulent natural convection in isothermal rectangular flat plates; Gonçalves et al. (2021), in the experimental study of machining with different cutting fluids under convection conditions with phase change, correlating the parameters Leidenfrost temperature, cooling capacity and machining temperature; and Verdério Júnior et al. (2021c), in proposing a dimensionless physical-mathematical methodology for the study of turbulent natural convection, using the $\kappa - \varepsilon$ and $\kappa - \omega$ SST turbulence models.

This work aims to present an experimental methodology for studying natural convection over flat and corrugated plates. This methodology reaches from the design and construction of the physical apparatus to the development of a physical-mathematical formulation to determine the main physical parameters associated with the phenomenon, including the study for the analysis and propagation of uncertainties. The final formulation will serve as a subsidy for future studies, experimental and numerical-experimental, of the process of natural convection heat transfer, in the most diverse applications of Thermal Engineering.

MATERIALS AND METHODS

Design and Construction of the Experimental Apparatus

To study the process of natural convection cooling on plates (flat or corrugated), it is necessary, before obtaining a suitable physical-mathematical formulation, the design and construction of the experimental apparatus to be used.

The first stage comprises manufacturing the studied plates, which can be obtained through manufacturing processes by machining or mechanical forming. The use of aluminum alloys as raw material for the plates is a very viable option, since despite the higher acquisition costs, they have high thermal conductivity – which makes heating and cooling processes faster and more efficient, reducing costs associated – and mechanical properties that provide

lower costs and shorter times demanded in the mechanical manufacturing process. The measurement of the final geometric characteristics of the plates and the physical properties of the material used (such as specific heat capacity and average emissivity) occurs at this stage; highlighting that the degree of precision and accuracy of the measurement tools used will influence the uncertainty analysis process.

After manufacturing the plates, there is the design and construction of the temperature measuring apparatus, as well as the selection of the data acquisition system. Several types of sensors can be used to measure temperatures; such as the DS18B20, platinum resistance temperature detector (RTD Pt100) or TMP117 high-precision digital temperature sensor. These sensors will be responsible for capturing the evolution of temperatures with the time in the different regions of the plate studied and in the free-stream environment during the cooling process.

Different ways of construction the temperature measuring apparatus are possible, with different possibilities for positioning the sensors on the plate and in the free-stream environment; that will be determined according to the objectives of the experiment in planning and that will influence the characteristics and the programming of the data acquisition system to be used. The resulting temperature measuring apparatus must be positioned in the central region of a large chamber and thermally isolated from the external environment – which reduces the influence of wall effects on the flow and enables a plate cooling process predominantly by natural convection, although the portion of thermal radiation heat transfer is still considerable.

After manufacturing the plates and constructing the temperature measurement apparatus, there are the steps of the heating and cooling process of the plate. The maximum heating temperature will be determined by observing the melting temperature of the material of the plates and the range of interest of the Rayleigh number for the study of the heat transfer process by natural convection.

After heating and homogenizing the temperatures of the plate inside the furnace, the heated plate is quickly transferred to the temperature measuring apparatus in the cooling chamber isolated from the external environment; where it will remain until the end of the cooling process. During transferring the plate to the controlled environment, external disturbances and heat losses occur in the cooling process. Thus, it is necessary to wait a period for the homogenization of temperatures in the plate region, so that, only after this stabilization period, the analysis of the transient exponential decay curve of the cooling process by natural convection can be performed. The homogenization time (t_{eq}) is obtained from the qualitative visual graphic analysis of the temporal distribution of temperatures for the sensors used.

Figure 1 schematically illustrates a possible arrangement of the temperature measuring apparatus and its positioning inside the experimental cooling chamber. In this form of construction, the temperature sensors are placed on the upper face of an MDF wooden support box – coated on the side with insulating styrofoam and filled with high-density insulating foam. Temperature measurement will take place at different positions in the lower region of the plate, through direct pressure contact with the sensors; with emphasis on the use of the thermal paste to improve the heat transfer process from the plate to the sensors and to reduce the influence of external elements (such as air trapped between the spacing of the plate and the sensors). There is also the use of an additional sensor to measure the ambient free-stream temperature, located in a position further away from the disturbance region on the plate. All temperature sensors (under the plate and in the environment) are interconnected in a guide cable, which connects to a data acquisition system for further processing and analysis of results.

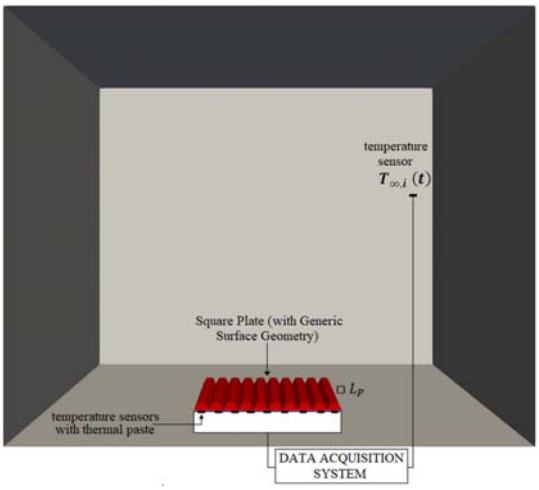

Figure 1. Schematic graphic representation of a form of construction of the Experimental Apparatus.

To increase the statistical representativeness of the results obtained, it is necessary to repeat the heating, controlled cooling, and data collection for each plate geometry studied at least three (03) times.

Figure 2 illustrates the stages of the proposed experimental methodology for studying the process of natural convection heat transfer on the plates in a sequential schematic form.

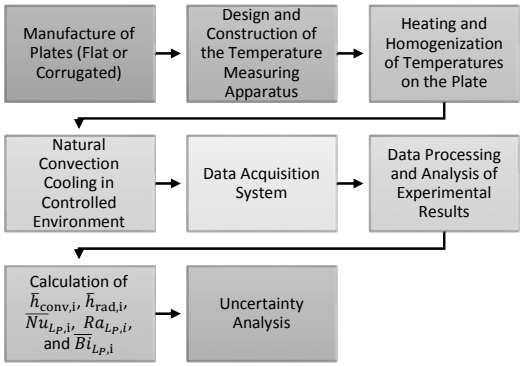

Figure 2. Sequence of steps of the proposed methodology for the experimental study of natural convection on flat or corrugated plates.

Methodology of data processing and analysis of experimental results

The methodology for calculating the physical parameters of the heat transfer process by natural convection over plates (flat or corrugated) begins with the processing and analysis of the collected experimental results.

Assuming a uniform three-dimensional distribution of temperatures across the surface of the studied plate at each instant of time – a valid hypothesis for bodies of small dimensions, with high thermal conductivity and immersed in a medium with low thermal conductivity (such as air) and stationary or with low movement speed – there is the application of the Lumped Capacitance Method, by Incropera et al. (2008), Cengel and Ghajar (2012) and Kreith et al. (2014), which presents errors of the order of 5% for $Bi \leq 0.1$.

The designed experimental apparatus has N sensors to capture transient temperatures in the plate region and one (01) sensor to measure the ambient free-stream temperature.

The application of the Lumped Capacitance Method implies a uniform distribution of temperatures, in each instant of time, in the plate region. To better approximate the experimental behavior of the data obtained with this physical hypothesis, a linear calibration procedure is applied to the sensors in the region of the plate and the data before the stabilization of readings, with $t < t_{eq}$, are discarded.

Linear calibration aims to improve the uniformity of temperature readings of the sensors in contact with the plate at each instant of time. This procedure consists of obtaining and applying a linear regression equation for each sensor in the plate region, interrelating the average temperature of all N sensors and the individual readings of each sensor for each instant of time.

After the linear calibration procedure, the results obtained before the time interval necessary to stabilize the temperature readings of the N sensors on the plate are eliminated. This step aims at a proper analysis of the behavior of the exponential transient decay of the temperature curves on the board, which occurs only after the linear calibration of the sensors' measurements on the board and under conditions of $t \geq t_{eq}$.

For each plate and in each assay studied, the resulting transient temperature curve is calculated through the simple arithmetic average of the calibrated measurements of the N sensors in contact with the plate after the period of stabilization of readings in each performed test.

For each different plate geometry studied, at least three (03) tests will be performed, subdivided into i intervals; each one with temperature variations (ΔT) of specified order according to the intervals of the Rayleigh number studied and the objectives of the experiment.

Figure 3 schematically illustrates the steps in the methodology for processing and analyzing results.

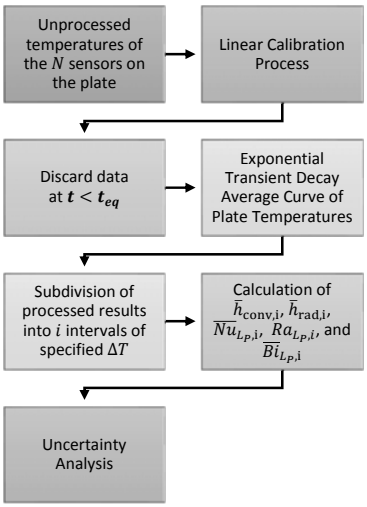

Figure 3. Sequence of steps of the methodology for processing and analysis of experimental results.

PHYSICAL-MATHEMATICAL MODELING

After the previous steps, the physical-mathematical modeling is formulated to be applied to the experimental data obtained and processed.

From the Lumped Capacitance Method:

$$\frac{T - T_\infty}{T_{initial} - T_\infty} = \exp\left[-\left(\frac{\bar{h}_{total}.A}{m_P.c_{Al}}\right).t\right] = \exp[-(C_t).t] \qquad (1)$$

$$\frac{\bar{h}_{total}.A}{m_P.c_{Al}} = C_t \qquad (2)$$

The term C_t is the empirical coefficient of the exponential interpolation curve of the experimental data of the dimensionless equation of temperatures as a function of time. This term is calculated through exponential numerical curve fitting methods, for each time interval considered and in each test performed.

Several simplifying hypotheses, approximations, and physical definitions are applied to the problem understudy in the modeling process. That are:

- The surface of the plates behaves like a small gray body inside an extensive neighborhood, with $Q_{rad} = \bar{h}_{rad}.A_P.(T_S - T_{nb})$;
- $T_\infty \cong T_{nb}$;
- Newton's law of cooling, with $Q_{conv} = \bar{h}_{conv}.A.(T_S - T_\infty)$;
- The thermal properties of solid c_{Al} and $k_{t_{Al}}$, in the temperature range of the experiments performed, present low variation and can be assumed to be approximately constants;
- $\bar{h}_{total} = \bar{h}_{conv} + \left(\frac{A_P}{A}\right).\bar{h}_{rad}$, considering the thermal radiation heat exchanges between the surfaces and corrugations of the plate itself and with the external environment;
- $\bar{h}_{rad} = \varepsilon.\sigma.(T_s + T_{nb}).(T_S^2 + T_{nb}^2)$;
- $T_{initial} = T(t = t_{initial})$, $T_{final} = T(t = t_{final})$ and $\Delta t = t_{final} - t_{initial}$, for each time interval considered in each test performed.

Through physical definitions, substitutions and mathematical manipulations in Equation (1), there is:

$$\bar{h}_{conv} = \frac{C_t.m_P.c_{Al}}{A} - \left(\frac{A_P}{A}\right).\varepsilon.\sigma.(T_s + T_\infty).(T_s^2 + T_\infty^2) \quad (3)$$

The average convective heat transfer coefficient, $\bar{h}_{conv}$, i, is evaluated for each time interval considered in each test performed.

The plate surface temperature can be approximated as the simple arithmetic average of the initial and final temperatures within the time interval considered, so that:

$$\overline{T}_{s,i} = \frac{\overline{T}_{initial,i} + \overline{T}_{final,i}}{2} \quad (4)$$

The initial temperature $\left(\overline{T}_{initial,i}\right)$ and final temperature $\left(\overline{T}_{final,i}\right)$ are calculated through the simple arithmetic average of the calibrated measurements of the N sensors on the plate at the initial and final instants, respectively. The free-stream temperature of the medium $\left(\overline{T}_{\infty,i}\right)$, disregarding small variations over time, is calculated as the simple arithmetic average of the temperatures measured by the specific sensor during the considered time interval.

Rewriting and rearranging Equation (3) through introducing the index i in the time interval and defining the initial, final and free-stream temperatures, there is:

$$\bar{h}_{conv,i} = \frac{C_{t,i}.m_P.c_{Al}}{A} - \left(\frac{A_P}{A}\right).\varepsilon.\sigma. \cdot\left(\left(\frac{\overline{T}_{initial,i} + \overline{T}_{final,i}}{2}\right) + \overline{T}_{\infty,i}\right). \cdot\left(\left(\frac{\overline{T}_{initial,i} + \overline{T}_{final,i}}{2}\right)^2 + \overline{T}_{\infty,i}^2\right) \quad (5)$$

The average thermal radiation heat transfer coefficient $\left(\bar{h}_{rad,i}\right)$ can be obtained from its definition, so that:

$$\bar{h}_{rad,i} = \varepsilon.\sigma.\left(\left(\frac{\overline{T}_{initial,i} + \overline{T}_{final,i}}{2}\right) + \overline{T}_{\infty,i}\right). \cdot\left(\left(\frac{\overline{T}_{initial,i} + \overline{T}_{final,i}}{2}\right)^2 + \overline{T}_{\infty,i}^2\right) \quad (6)$$

From the definition of the average Nusselt number, according to Incropera et al. (2008), using the plate longitudinal length (L_P) as a characteristic dimension of the flow studied and rearranging Equation (5), there is:

$$\overline{Nu}_{L_P,i} = \frac{C_{t,i}.m_P.c_{Al}.L_P}{A.k_{t_{fluid}}} - \left(\frac{A_P}{A}\right)\frac{\varepsilon.\sigma.L_P}{k_{t_{fluid}}}\left(\left(\frac{\overline{T}_{initial,i} + \overline{T}_{final,i}}{2}\right) + \overline{T}_{\infty,i}\right). \cdot\left(\left(\frac{\overline{T}_{initial,i} + \overline{T}_{final,i}}{2}\right)^2 + \overline{T}_{\infty,i}^2\right) \quad (7)$$

, which is used to evaluate $\overline{Nu}_{L_P,i}$ in each time interval considered and for each test performed.

The Rayleigh number for each time interval of each test performed – according to Incropera et al. (2008) and through the approximation adopted for the calculation of the surface temperature of Equation (4) – can be calculated through the Equation:

$$Ra_{L_P,i} = \frac{|\mathbf{g}|.\left(\frac{1}{\overline{T}_{f,i}}\right)\left(\frac{\overline{T}_{initial,i} + \overline{T}_{final,i}}{2} - \overline{T}_{\infty,i}\right)L_P^3}{\nu^2}.Pr \quad (8)$$

Where $\overline{T}_{f,i}$ is the average boundary layer temperature or film temperature, which is given by:

$$\overline{T}_{f,i} = \frac{\overline{T}_{s,i} + \overline{T}_{\infty,i}}{2} = \left(\frac{\frac{\overline{T}_{initial,i} + \overline{T}_{final,i}}{2} + \overline{T}_{\infty,i}}{2}\right) \quad (9)$$

The properties ν, $k_{t_{fluid}}$, and Pr of the air tend to present low variation in the temperature range of the experiments performed. Thus, they can be assumed to be approximately constant in each test performed and are evaluated in the corresponding $\overline{T}_{f,i}$ of the respective test.

Finally, to validate the application of the Lumped Capacitance Method for each time interval of each test performed, the Biot number is calculated. From its definition by Incropera et al. (2008) and of Equation (2), there is:

$$\mathrm{Bi}_{\mathrm{L_P,i}} = \frac{\mathrm{C_{t,i}}.\,\mathrm{m_P}.\,\mathrm{c_{Al}}.\,\mathrm{L_P}}{\mathrm{A}.\,\mathrm{k_{t_{Al}}}} \tag{10}$$

UNCERTAINTY ANALYSIS

The final step of the proposed methodology consists of the uncertainty analysis of the dimensionless groups of the $\overline{\mathrm{Nu}}_{\mathrm{L_P,i}}$, $\mathrm{Ra}_{\mathrm{L_P,i}}$ and $\mathrm{Bi}_{\mathrm{L_P,i}}$; according to references by Kline and McClinktock (1953) and Holman (2011).

From Equation (7), the $\overline{\mathrm{Nu}}_{\mathrm{L_P,i}}$ is function of $\mathrm{C_{t,i}}, \mathrm{m_P}, \mathrm{c_{Al}}, \mathrm{L_P}, \mathrm{A}, \mathrm{A_P}, \mathrm{k_{t_{fluid}}}, \varepsilon, \sigma, \overline{\mathrm{T}}_{\infty,\mathrm{i}}, \overline{\mathrm{T}}_{\mathrm{initial,i}}$, and $\overline{\mathrm{T}}_{\mathrm{final,i}}$. Thus, the estimation of the propagation of uncertainties about the $\overline{\mathrm{Nu}}_{\mathrm{L_P,i}}$ can be calculated through:

$$\begin{aligned}\delta^2_{\overline{\mathrm{Nu}}_{\mathrm{L_P,i}}} = &\left(\frac{\partial\overline{\mathrm{Nu}}_{\mathrm{L_P,i}}}{\partial \mathrm{C_{t,i}}}\right)^2\delta^2_{\mathrm{C_{t,i}}} + \left(\frac{\partial\overline{\mathrm{Nu}}_{\mathrm{L_P,i}}}{\partial \mathrm{m_P}}\right)^2\delta^2_{\mathrm{m_P}} + \\ &+\left(\frac{\partial\overline{\mathrm{Nu}}_{\mathrm{L_P,i}}}{\partial \mathrm{c_{Al}}}\right)^2\delta^2_{\mathrm{c_{Al}}} + \left(\frac{\partial\overline{\mathrm{Nu}}_{\mathrm{L_P,i}}}{\partial \mathrm{L_P}}\right)^2\delta^2_{\mathrm{L_P}} + \\ &+\left(\frac{\partial\overline{\mathrm{Nu}}_{\mathrm{L_P,i}}}{\partial \mathrm{A}}\right)^2\delta^2_{\mathrm{A}} + \left(\frac{\partial\overline{\mathrm{Nu}}_{\mathrm{L_P,i}}}{\partial \mathrm{A_P}}\right)^2\delta^2_{\mathrm{A_P}} + \\ &+\left(\frac{\partial\overline{\mathrm{Nu}}_{\mathrm{L_P,i}}}{\partial \mathrm{k_{t_{fluid}}}}\right)^2\delta^2_{\mathrm{k_{t_{fluid}}}} + \left(\frac{\partial\overline{\mathrm{Nu}}_{\mathrm{L_P,i}}}{\partial \varepsilon}\right)^2\delta^2_{\varepsilon} + \\ &+\left(\frac{\partial\overline{\mathrm{Nu}}_{\mathrm{L_P,i}}}{\partial \sigma}\right)^2\delta^2_{\sigma} + \left(\frac{\partial\overline{\mathrm{Nu}}_{\mathrm{L_P,i}}}{\partial \overline{\mathrm{T}}_{\mathrm{initial,i}}}\right)^2\delta^2_{\overline{\mathrm{T}}_{\mathrm{initial,i}}} + \\ &+\left(\frac{\partial\overline{\mathrm{Nu}}_{\mathrm{L_P,i}}}{\partial \overline{\mathrm{T}}_{\mathrm{final,i}}}\right)^2\delta^2_{\overline{\mathrm{T}}_{\mathrm{final,i}}} + \left(\frac{\partial\overline{\mathrm{Nu}}_{\mathrm{L_P,i}}}{\partial \overline{\mathrm{T}}_{\infty,\mathrm{i}}}\right)^2\delta^2_{\overline{\mathrm{T}}_{\infty,\mathrm{i}}}\end{aligned} \tag{11}$$

The individual terms of the partial derivatives of $\overline{\mathrm{Nu}}_{\mathrm{L_P,i}}$ are described in the equations below.

$$\frac{\partial\overline{\mathrm{Nu}}_{\mathrm{L_P,i}}}{\partial \mathrm{C_{t,i}}} = \frac{\mathrm{m_P}.\,\mathrm{c_{Al}}.\,\mathrm{L_P}}{\mathrm{A}.\,\mathrm{k_{t_{fluid}}}} \tag{12}$$

$$\frac{\partial\overline{\mathrm{Nu}}_{\mathrm{L_P,i}}}{\partial \mathrm{m_P}} = \frac{\mathrm{C_{t,i}}.\,\mathrm{c_{Al}}.\,\mathrm{L_P}}{\mathrm{A}.\,\mathrm{k_{t_{fluid}}}} \tag{13}$$

$$\frac{\partial\overline{\mathrm{Nu}}_{\mathrm{L_P,i}}}{\partial \mathrm{c_{Al}}} = \frac{\mathrm{C_{t,i}}.\,\mathrm{m_P}.\,\mathrm{L_P}}{\mathrm{A_s}.\,\mathrm{k_{t_{fluid}}}} \tag{14}$$

$$\begin{aligned}\frac{\partial\overline{\mathrm{Nu}}_{\mathrm{L_P,i}}}{\partial \mathrm{L_P}} = &\frac{1}{\mathrm{A}.\,\mathrm{k_{t_{fluid}}}}\left[\mathrm{C_{t,i}}.\,\mathrm{m_P}.\,\mathrm{c_{Al}}\right. \\ &\left.-\varepsilon.\,\sigma.\,\mathrm{A_P}\left(\left(\frac{\overline{\mathrm{T}}_{\mathrm{initial,i}}+\overline{\mathrm{T}}_{\mathrm{final,i}}}{2}\right)\overline{\mathrm{T}}_{\infty,\mathrm{i}}\right).\right. \\ &\left.\left(\left(\frac{\overline{\mathrm{T}}_{\mathrm{initial,i}}+\overline{\mathrm{T}}_{\mathrm{final,i}}}{2}\right)^2+\overline{\mathrm{T}}^2_{\infty,\mathrm{i}}\right)\right]\end{aligned} \tag{15}$$

$$\begin{aligned}\frac{\partial\overline{\mathrm{Nu}}_{\mathrm{L_P,i}}}{\partial \mathrm{A}} = &\frac{1}{\mathrm{A}^2.\,\mathrm{k_{t_{fluid}}}}\left[-\mathrm{C_{t,i}}.\,\mathrm{m_P}.\,\mathrm{c_{Al}}.\,\mathrm{L_P}\right. \\ &\left.+\mathrm{A_P}.\,\mathrm{L_P}.\,\varepsilon.\,\sigma.\left(\left(\frac{\overline{\mathrm{T}}_{\mathrm{initial,i}}+\overline{\mathrm{T}}_{\mathrm{final,i}}}{2}\right)+\overline{\mathrm{T}}_{\infty,\mathrm{i}}\right).\right. \\ &\left.\left(\left(\frac{\overline{\mathrm{T}}_{\mathrm{initial,i}}+\overline{\mathrm{T}}_{\mathrm{final,i}}}{2}\right)^2+\overline{\mathrm{T}}^2_{\infty,\mathrm{i}}\right)\right]\end{aligned} \tag{16}$$

$$\delta_{\mathrm{A}} = \sqrt{\left(\frac{\partial \mathrm{A}}{\partial \mathrm{L_P}}.\,\delta_{\mathrm{L_P}}\right)^2} = 2.\,\mathrm{L_P}.\,\delta_{\mathrm{L_P}} \tag{17}$$

$$\begin{aligned}\frac{\partial\overline{\mathrm{Nu}}_{\mathrm{L_P,i}}}{\partial \mathrm{A_P}} = &-\frac{\mathrm{L_P}.\,\varepsilon.\,\sigma}{\mathrm{A}.\,\mathrm{k_{t_{fluid}}}}. \\ &.\left(\left(\frac{\overline{\mathrm{T}}_{\mathrm{initial,i}}+\overline{\mathrm{T}}_{\mathrm{final,i}}}{2}\right)+\overline{\mathrm{T}}_{\infty,\mathrm{i}}\right). \\ &.\left(\left(\frac{\overline{\mathrm{T}}_{\mathrm{initial,i}}+\overline{\mathrm{T}}_{\mathrm{final,i}}}{2}\right)^2+\overline{\mathrm{T}}^2_{\infty,\mathrm{i}}\right)\end{aligned} \tag{18}$$

$$\delta_{\mathrm{A_P}} = \sqrt{\left(\frac{\partial \mathrm{A_P}}{\partial \mathrm{L_P}}\delta_{\mathrm{L_P}}\right)^2+\left(\frac{\partial \mathrm{A_P}}{\partial \mathrm{W}}\delta_{\mathrm{L_P}}\right)^2} = \sqrt{2}\mathrm{L_P}\delta_{\mathrm{L_P}} \tag{19}$$

$$\begin{aligned}\frac{\partial\overline{\mathrm{Nu}}_{\mathrm{L_P,i}}}{\partial \mathrm{k_{t_{fluid}}}} = &\frac{\mathrm{L_P}}{\mathrm{A}.\,\mathrm{k^2_{t_{fluid}}}}\left[-\mathrm{C_{t,i}}.\,\mathrm{m_P}.\,\mathrm{c_{Al}}+\mathrm{A_P}.\,\varepsilon.\,\sigma.\right. \\ &.\left(\left(\frac{\overline{\mathrm{T}}_{\mathrm{initial,i}}+\overline{\mathrm{T}}_{\mathrm{final,i}}}{2}\right)+\overline{\mathrm{T}}_{\infty,\mathrm{i}}\right). \\ &\left..\left(\left(\frac{\overline{\mathrm{T}}_{\mathrm{initial,i}}+\overline{\mathrm{T}}_{\mathrm{final,i}}}{2}\right)^2+\overline{\mathrm{T}}^2_{\infty,\mathrm{i}}\right)\right]\end{aligned} \tag{20}$$

$$\begin{aligned}\frac{\partial\overline{\mathrm{Nu}}_{\mathrm{L_P,i}}}{\partial \varepsilon} = &-\left(\frac{\mathrm{A_P}}{\mathrm{A}}\right)\frac{\sigma.\,\mathrm{L_P}}{\mathrm{k_{t_{fluid}}}}. \\ &.\left(\left(\frac{\overline{\mathrm{T}}_{\mathrm{initial,i}}+\overline{\mathrm{T}}_{\mathrm{final,i}}}{2}\right)+\overline{\mathrm{T}}_{\infty,\mathrm{i}}\right). \\ &.\left(\left(\frac{\overline{\mathrm{T}}_{\mathrm{initial,i}}+\overline{\mathrm{T}}_{\mathrm{final,i}}}{2}\right)^2+\overline{\mathrm{T}}^2_{\infty,\mathrm{i}}\right)\end{aligned} \tag{21}$$

$$\begin{aligned}\frac{\partial\overline{\mathrm{Nu}}_{\mathrm{L_P,i}}}{\partial \sigma} = &-\left(\frac{\mathrm{A_P}}{\mathrm{A}}\right)\frac{\varepsilon.\,\mathrm{L_P}}{\mathrm{k_{t_{fluid}}}}. \\ &.\left(\left(\frac{\overline{\mathrm{T}}_{\mathrm{initial,i}}+\overline{\mathrm{T}}_{\mathrm{final,i}}}{2}\right)+\overline{\mathrm{T}}_{\infty,\mathrm{i}}\right). \\ &.\left(\left(\frac{\overline{\mathrm{T}}_{\mathrm{initial,i}}+\overline{\mathrm{T}}_{\mathrm{final,i}}}{2}\right)^2+\overline{\mathrm{T}}^2_{\infty,\mathrm{i}}\right)\end{aligned} \tag{22}$$

$$\begin{aligned}\frac{\partial\overline{\mathrm{Nu}}_{\mathrm{L_P,i}}}{\partial \overline{\mathrm{T}}_{\mathrm{initial,i}}} = \frac{\partial\overline{\mathrm{Nu}}_{\mathrm{L_P,i}}}{\partial \overline{\mathrm{T}}_{\mathrm{final,i}}} = &-\left(\frac{\mathrm{A_P}}{\mathrm{A}}\right)\frac{\varepsilon.\,\sigma.\,\mathrm{L_P}}{8.\,\mathrm{k_{t_{fluid}}}} \\ &\left[3.\,\overline{\mathrm{T}}^2_{\mathrm{initial,i}}+6.\,\overline{\mathrm{T}}_{\mathrm{final,i}}.\,\overline{\mathrm{T}}_{\mathrm{initial,i}}+\right. \\ &+4.\,\overline{\mathrm{T}}_{\infty,\mathrm{i}}.\,\overline{\mathrm{T}}_{\mathrm{initial,i}}+3.\,\overline{\mathrm{T}}^2_{\mathrm{final,i}}+ \\ &\left.+4.\,\overline{\mathrm{T}}_{\infty,\mathrm{i}}.\,\overline{\mathrm{T}}_{\mathrm{final,i}}+4.\,\overline{\mathrm{T}}^2_{\infty,\mathrm{i}}\right]\end{aligned} \tag{23}$$

$$\begin{aligned}\frac{\partial\overline{\mathrm{Nu}}_{\mathrm{L_P,i}}}{\partial \overline{\mathrm{T}}_{\infty,\mathrm{i}}} = &-\left(\frac{\mathrm{A_P}}{\mathrm{A}}\right)\frac{\varepsilon.\,\sigma.\,\mathrm{L_P}}{4.\,\mathrm{k_{t_{fluid}}}}\left[\overline{\mathrm{T}}^2_{\mathrm{initial,i}}+\right. \\ &+2.\,\overline{\mathrm{T}}_{\mathrm{final,i}}.\,\overline{\mathrm{T}}_{\mathrm{initial,i}}+4.\,\overline{\mathrm{T}}_{\infty,\mathrm{i}}.\,\overline{\mathrm{T}}_{\mathrm{initial,i}}+ \\ &\left.+\overline{\mathrm{T}}^2_{\mathrm{final,i}}++4.\,\overline{\mathrm{T}}_{\infty,\mathrm{i}}.\,\overline{\mathrm{T}}_{\mathrm{final,i}}+12.\,\overline{\mathrm{T}}^2_{\infty,\mathrm{i}}\right]\end{aligned} \tag{24}$$

In turn, according to Equation (8), $\mathrm{Ra_{L_P,i}} = \mathrm{f}\left(\mathbf{g}, \mathrm{L_P}, \mathrm{Pr}, \nu, \overline{\mathrm{T}}_{\mathrm{initial,i}}, \overline{\mathrm{T}}_{\mathrm{final,i}}, \overline{\mathrm{T}}_{\infty,\mathrm{i}}\right)$. The propaga-tion of uncertainties in this term occurs through the equation:

$$\begin{aligned}\delta^2_{\mathrm{Ra_{L_P,i}}} = &\left(\frac{\partial \mathrm{Ra_{L_P,i}}}{\partial \mathbf{g}}\right)^2 \delta^2_{\mathbf{g}} + \left(\frac{\partial \mathrm{Ra_{L_P,i}}}{\partial \mathrm{L_P}}\right)^2 \delta^2_{\mathrm{L_P}} + \\ &+ \left(\frac{\partial \mathrm{Ra_{L_P,i}}}{\partial \mathrm{Pr}}\right)^2 \delta^2_{\mathrm{Pr}} + \left(\frac{\partial \mathrm{Ra_{L_P,i}}}{\partial \nu}\right)^2 \delta^2_{\nu} + \\ &+ \left(\frac{\partial \mathrm{Ra_{L_P,i}}}{\partial \overline{\mathrm{T}}_{\mathrm{initial,i}}}\right)^2 \delta^2_{\overline{\mathrm{T}}_{\mathrm{initial,i}}} + \left(\frac{\partial \mathrm{Ra_{L_P,i}}}{\partial \overline{\mathrm{T}}_{\mathrm{final,i}}}\right)^2 \delta^2_{\overline{\mathrm{T}}_{\mathrm{final,i}}} \\ &+ \left(\frac{\partial \mathrm{Ra_{L_P,i}}}{\partial \overline{\mathrm{T}}_{\infty,\mathrm{i}}}\right)^2 \delta^2_{\overline{\mathrm{T}}_{\infty,\mathrm{i}}}\end{aligned} \tag{25}$$

The individual terms of the partial derivatives of $\mathrm{Ra_{L_P,i}}$ are described in the following equations:

$$\frac{\partial \mathrm{Ra_{L_P,i}}}{\partial \mathbf{g}} = \frac{2.\mathrm{L_P^3}.\mathrm{Pr}.\left(\overline{\mathrm{T}}_{\mathrm{initial,i}} + \overline{\mathrm{T}}_{\mathrm{final,i}} - 2.\overline{\mathrm{T}}_{\infty,\mathrm{i}}\right)}{\left(\overline{\mathrm{T}}_{\mathrm{initial,i}} + \overline{\mathrm{T}}_{\mathrm{final,i}} + 2.\overline{\mathrm{T}}_{\infty,\mathrm{i}}\right).\nu^2} \tag{26}$$

$$\frac{\partial \mathrm{Ra_{L_P,i}}}{\partial \mathrm{L_P}} = \frac{6.|\mathbf{g}|.\mathrm{L_P^2}.\mathrm{Pr}.\left(\overline{\mathrm{T}}_{\mathrm{initial,i}} + \overline{\mathrm{T}}_{\mathrm{final,i}} - 2.\overline{\mathrm{T}}_{\infty,\mathrm{i}}\right)}{\left(\overline{\mathrm{T}}_{\mathrm{initial,i}} + \overline{\mathrm{T}}_{\mathrm{final,i}} + 2.\overline{\mathrm{T}}_{\infty,\mathrm{i}}\right).\nu^2} \tag{27}$$

$$\frac{\partial \mathrm{Ra_{L_P,i}}}{\partial \mathrm{Pr}} = \frac{2.|\mathbf{g}|.\mathrm{L_P^3}.\left(\overline{\mathrm{T}}_{\mathrm{initial,i}} + \overline{\mathrm{T}}_{\mathrm{final,i}} - 2.\overline{\mathrm{T}}_{\infty,\mathrm{i}}\right)}{\left(\overline{\mathrm{T}}_{\mathrm{initial,i}} + \overline{\mathrm{T}}_{\mathrm{final,i}} + 2.\overline{\mathrm{T}}_{\infty,\mathrm{i}}\right).\nu^2} \tag{28}$$

$$\frac{\partial \mathrm{Ra_{L_P,i}}}{\partial \nu} = -\frac{4.|\mathbf{g}|.\mathrm{L_P^3}.\mathrm{Pr}\left(\overline{\mathrm{T}}_{\mathrm{initial,i}} + \overline{\mathrm{T}}_{\mathrm{final,i}} - 2.\overline{\mathrm{T}}_{\infty,\mathrm{i}}\right)}{\left(\overline{\mathrm{T}}_{\mathrm{initial,i}} + \overline{\mathrm{T}}_{\mathrm{final,i}} + 2.\overline{\mathrm{T}}_{\infty,\mathrm{i}}\right).\nu^3} \tag{29}$$

$$\frac{\partial \mathrm{Ra_{L_P,i}}}{\partial \overline{\mathrm{T}}_{\mathrm{initial,i}}} = \frac{\partial \mathrm{Ra_{L_P,i}}}{\partial \overline{\mathrm{T}}_{\mathrm{final,i}}} = \frac{8.|\mathbf{g}|.\mathrm{L_P^3}.\mathrm{Pr}.\overline{\mathrm{T}}_{\infty,\mathrm{i}}}{\left(\overline{\mathrm{T}}_{\mathrm{initial,i}} + \overline{\mathrm{T}}_{\mathrm{final,i}} + 2.\overline{\mathrm{T}}_{\infty,\mathrm{i}}\right).\nu^2} \tag{30}$$

$$\frac{\partial \mathrm{Ra_{L_P,i}}}{\partial \overline{\mathrm{T}}_{\infty,\mathrm{i}}} = -\frac{8.|\mathbf{g}|.\mathrm{L_P^3}.\mathrm{Pr}.\left(\overline{\mathrm{T}}_{\mathrm{initial,i}} + \overline{\mathrm{T}}_{\mathrm{final,i}}\right)}{\left(\overline{\mathrm{T}}_{\mathrm{initial,i}} + \overline{\mathrm{T}}_{\mathrm{final,i}} + 2.\overline{\mathrm{T}}_{\infty,\mathrm{i}}\right)^2.\nu^2} \tag{31}$$

Finally, there is the analysis of propagation of uncertainties in the term $\mathrm{Bi_{L_P,i}}$, which according to equation (10), is a function of $\mathrm{C_{t,i}}, \mathrm{m_P}, \mathrm{c_{Al}}, \mathrm{L_P}, \mathrm{A}$ and $\mathrm{k_{t_{Al}}}$. There is:

$$\begin{aligned}\delta^2_{\mathrm{Bi_{L_P,i}}} = &\left(\frac{\partial \mathrm{Bi_{L_P,i}}}{\partial \mathrm{C_{t,i}}}\right)^2 \delta^2_{\mathrm{C_{t,i}}} + \left(\frac{\partial \mathrm{Bi_{L_P,i}}}{\partial \mathrm{m_P}}\right)^2 \delta^2_{\mathrm{m_P}} + \\ &+ \left(\frac{\partial \mathrm{Bi_{L_P,i}}}{\partial \mathrm{c_{Al}}}\right)^2 \delta^2_{\mathrm{c_{Al}}} + \left(\frac{\partial \mathrm{Bi_{L_P,i}}}{\partial \mathrm{L_P}}\right)^2 \delta^2_{\mathrm{L_P}} + \\ &+ \left(\frac{\partial \mathrm{Bi_{L_P,i}}}{\partial \mathrm{A}}\right)^2 \delta^2_{\mathrm{A}} + \left(\frac{\partial \mathrm{Bi_{L_P,i}}}{\partial \mathrm{k_{t_{Al}}}}\right)^2 \delta^2_{\mathrm{k_{t_{Al}}}}\end{aligned} \tag{32}$$

The individual terms of the partial derivatives of $\mathrm{Bi_{L_P,i}}$ are described in the following equations:

$$\frac{\partial \mathrm{Bi_{L_P,i}}}{\partial \mathrm{C_{t,i}}} = \frac{\mathrm{m_P}.\mathrm{c_{Al}}.\mathrm{L_P}}{\mathrm{A}.\mathrm{k_{t_{Al}}}} \tag{33}$$

$$\frac{\partial \mathrm{Bi_{L_P,i}}}{\partial \mathrm{m_P}} = \frac{\mathrm{C_{t,i}}.\mathrm{c_{Al}}.\mathrm{L_P}}{\mathrm{A}.\mathrm{k_{t_{Al}}}} \tag{34}$$

$$\frac{\partial \mathrm{Bi_{L_P,i}}}{\partial \mathrm{c_{Al}}} = \frac{\mathrm{C_{t,i}}.\mathrm{m_P}.\mathrm{L_P}}{\mathrm{A}.\mathrm{k_{t_{Al}}}} \tag{35}$$

$$\frac{\partial \mathrm{Bi_{L_P,i}}}{\partial \mathrm{L_P}} = \frac{\mathrm{C_{t,i}}.\mathrm{m_P}.\mathrm{c_{Al}}}{\mathrm{A}.\mathrm{k_{t_{Al}}}} \tag{36}$$

$$\frac{\partial \mathrm{Bi_{L_P,i}}}{\partial \mathrm{A}} = -\frac{\mathrm{C_{t,i}}.\mathrm{m_P}.\mathrm{c_{Al}}.\mathrm{L_P}}{\mathrm{A^2}.\mathrm{k_{t_{Al}}}} \tag{37}$$

$$\frac{\partial \mathrm{Bi_{L_P,i}}}{\partial \mathrm{k_{t_{Al}}}} = -\frac{\mathrm{C_{t,i}}.\mathrm{m_P}.\mathrm{c_{Al}}.\mathrm{L_P}}{\mathrm{A}.\mathrm{k_{t_{Al}}^2}} \tag{38}$$

DISCUSSIONS AND CONCLUSIONS

The present work presented an experimental methodology for studying natural convection on flat and corrugated plates. The steps of design and construction of the experimental apparatus and data processing and analysis were discussed in detail, followed by applying the Lumped Capacitance Method (and other physical equations and concepts) in the deduction of a physical-mathematical model applicable to the objectives of the proposed methodology. In the end, the formulation of the procedure for analysis and propagation of uncertainties was meticulously deduced in alignment with the proposed methodology objectives.

The proposed methodology can be extended to the most diverse applications of the study of natural convection, both in the applied industry environment and in the academic research environment.

An application of the proposed methodology is to obtain empirical relations of the type $\overline{Nu}_{L_P}$ x Ra_{L_P}, $\bar{h}_{\mathrm{conv}}$ x Ra_{L_P}, $\bar{h}_{\mathrm{rad}}$ x ΔT, etc. for different plate geometries and in conditions of the high spectrum and higher values of the Rayleigh number. Such empirical results are widely used and extremely important in the experimental validation of numerical models and methodologies; as presented in the numerical-experimental validation studies by Verdério Júnior et al. (2021a) and Verdério Júnior et al. (2021b). Similarly, these empirical results can support the formulation of other experimental methodologies and also as well as the design and optimization of measurement instruments. It is important to highlight that the design and construction characteristics of the experimental apparatus will determine the ranges of the Rayleigh number that can be reached experimentally.

Another application of the different types of empirical results of the proposed experimental methodology refers to sensitivity analysis studies about the uncertainties propagated through the various measuring instruments. Such studies would demonstrate the biggest bottlenecks responsible for the propagation of measurement uncertainties and point out optimization alternatives for the design of the experimental apparatus.

The experimental methodology developed in this work will appear in the current scientific literature as a technical-scientific manual to support the empirical study of natural convection - reaching

from the design and construction of the physical apparatus to the physical-mathematical modeling of determination the main physical parameters associated with the phenomenon.

The physical-mathematical modeling of the experimental methodology applied to the problem-situation studied, despite presenting high accuracy, has limitations of accuracy; with minimum errors of the order of 5% under conditions of $Bi \leq 0.1$. Thus, the use of other forms of modeling the problem-situation is an alternative to be studied, aiming to obtain results with even greater accuracy.

As other references to future works, the following proposals are highlighted.

Adapt the developed methodology to forced convection problems, with phase change and/or with thermal radiation heat transfer in participating medium.

To perform numerical computational simulations of the natural convection process and, together with the proposed experimental methodology, use an infrared camera for the quantitative and qualitative study of the transient cooling process. In the end, from the results obtained, validate and/or calibrate the proposed physical-numerical model.

ACKNOWLEDGEMENTS

The authors thank to Instituto Federal de Educação, Ciência e Tecnologia de São Paulo (IFSP), Araraquara campus and Catanduva campus; to Universidade Estadual Paulista "Júlio de Mesquita Filho" (UNESP), Faculdade de Engenharia (FEB), Bauru campus; and to research group ENACO (Energia e Aplicações Correlatas) for providing the workforce and the conditions to produce this research project.

REFERENCES

Balaji, C., Srinivasanet, B., and Gedupudi, S., 2021, *Chapter 6 – Natural convection*, Heat Transfer Engineering, Fundamentals and Techniques, Academic Press, ISBN: 9780128185032, p. 173-198. DOI: https://doi.org/10.1016/B978-0-12-818503-2.00006-X.

Bejan, A., 2013, *Convection Heat Transfer*, John wiley & Sons.

Bergman, T. L. et al., 2014, *Fundamentos da Transferência de Calor e de Massa*, LTC (*in Portuguese*).

Çengel, Y. A., and Ghajar, A. J., 2012, *Transferência de Calor e Massa: Uma abordagem prática*, AMGH (*in Portuguese*).

Fishenden, M., and Saunders, O., 1965, *An Introduction to Heat Transfer*, Clarendon Press, Oxford.

Frank, A., Heidemann, W. and Spindler, K. 2019, *Electronic Component Cooling Inside Switch Cabinets: Combined Radiation and Natural Convection Heat Transfer*, Heat Mass Transfer, Vol. 55, pp. 699–709.

Gonçalves, D. M., Sanchez, L. E. A., and Verdério Júnior, S. A., 2021, *Correlation between Leidenfrost Temperature, Cooling Capacity snd Machining Temperature: An Experimental Study of Cutting Fluids*, Revista de Engenharia Térmica, Vol. 20, No. 3, p. 10-15. DOI: http://dx.doi.org/10.5380/reterm.v20i3.83264.

Holman, J. P., 2011, *Experimental Methods for Engineers*, McGraw-Hill Science/Engineering/Math.

Incropera, F. et al., 2008, *Fundamentos da Transferência de Calor e de Massa*, LTC (*in Portuguese*).

Izadi, M., and Assad, M. E. H., 2021, *Chapter 15 – Use of nanofluids in solar energy systems,* Design and Performance Optimization of Renewable Energy Systems, Academic Press, ISBN: 9780128216026, p. 221-250. DOI: https://doi.org/10.1016/B978-0-12-821602-6.00017-1.

Kitamura, K., Mitsuishi, A., Suzuki, T. and Kimura, F., 2015, *Fluid Flow and Heat Transfer of Natural Convection Adjacent to Upward-Facing, Rectangular Plates of Arbitrary Aspect Ratios*, International Journal of Heat and Mass Transfer, Vol. 89, pp. 320–332.

Kline, S. J., and McClintock, F. A., 1953, *Describing uncertainties in single-sample experiments,* Mechanical Engineering, Vol. 75, p. 3–8.

Kreith, F., Manglik, R. M., and Bohn, M. S., 2014, *Princípios de Transferência de Calor*, Cengage Learning (*in Portuguese*).

Saha, S. C., Gu, Y. T., and Khan, M. M. K., 2016, *Chapter 3 – Natural Convection Heat Transfer in the Partitioned Attic Space*, Thermofluid Modeling for Energy Efficiency Applications, Academic Press, ISBN: 9780128023976, p. 59-72. DOI: https://doi.org/10.1016/B978-0-12-802397-6.00003-8.

Sheikholeslami, M., 2019, *Chapter 7 – Effect of Uniform Lorentz Forces on Nanofluid Flow Using CVFEM*, Application of Control Volume Based Finite Element Method (CVFEM) for Nanofluid Flow and Heat Transfer, Micro and Nano Technologies, Elsevier, ISBN: 9780128141526, p. 163-199. DOI: https://doi.org/10.1016/B978-0-12-814152-6.00007-2.

Silva, V. R. et al., 2021, *Study and Validation of meshes in turbulent isothermal problems of natural convection in flat plates*, Revista de Engenharia Térmica, Vol. 20, No. 2, p. 33-40. DOI: http://dx.doi.org/10.5380/reterm.v20i2.81785.

Verdério Júnior, S. A. et al., 2021a, *Physical–numerical parameters in turbulent simulations of natural convection on three-dimensional square plates*, International Journal of Numerical Methods for Heat & Fluid Flow, Vol. 3, No 2, p. 761–784. DOI: https://doi.org/10.1108/HFF-02-2021-0128.

Verdério Júnior, S. A., Scalon, V. L., and Oliveira, S. R., 2021b, *Physical–numerical parameters in laminar simulations of natural convection on three-dimensional square plates*, International Journal of Numerical Methods for Heat & Fluid Flow. DOI: https://doi.org/10.1108/HFF-07-2021-0478.

Verdério Júnior, S. A. et al., 2021c, *Dimensionless Physical-Mathematical Modeling of Turbulent Natural Convection*, Revista de Engenharia Térmica, Vol. 20, No. 3, p. 37-43. DOI: http://dx.doi.org/10.5380/reterm.v20i3.83269.